

ELECTRON MICROSCOPY ANALYSIS OF SEMI-COKE FROM THE MICROWAVE PYROLYSIS OF OIL SHALE WITH ITS FRACTAL DESCRIPTION

WANG QING*, LIU TONG, LIU HONGPENG, QIN HONG,
LI SHAOHUA

Northeast Dianli University
Jilin 132012, China

This paper discusses the potential use of microwave technology as an energy-efficient alternative to current heating technologies employed for treatment of Jilin Huadian oil shale and analyzes the surface pore structure of its semi-coke particle by a scanning electron microscope (SEM). The fractal theory was introduced into Scanning Electron Microscopy image analysis, and the particle surface fractal dimension (D) was used to describe quantitatively the surface character of oil shale/semi-coke particles. The SEM image was transformed into fractal one and the fractal dimensions were figured out with the box-counting approach. According to adsorption isotherm data, FHH model approach was also used to calculate the surface fractal dimension. Then, the box-counting approach was corroborated by using FHH model approach. It means that the fractal pore structure characteristics of samples could be described by a box-counting approach. Meanwhile, the results also showed that the microwave pyrolysis technology had a notable impact on the pore structure of samples.

Introduction

The importance of oil shale (OS) as a source of energy and as a chemical feedstock is well known. The lack of appreciable crude oil reserves encourages some countries to develop alternative energy sources, for example, synthetic oil from coal and other fossil fuels, and in this perspective OS could be as important as coal. Therefore, in recent years, many studies have been conducted on OS in those countries having an abundance of this resource, e.g. USA, Estonia, China and Australia [1]. China is one of the countries in the world where oil shale resources are great, and shale is suitable for large-scale exploitation and comprehensive utilization. China's deposits are distributed mainly in Maoming, Hadean, Fushun, Longkou, etc. [2]. Oil shale in

* Corresponding author: e-mail rlx888@126.com

Huadian deposit is of high grade and suitable for comprehensive exploration which includes oil shale mining, retorting, semi-coke (SC) combustion and production of building materials [3].

OS can be exploited by two main processes: a) extraction of the organic part – kerogen – by pyrolysis in retorts to obtain shale oil, b) direct combustion [4]. Organic fractions of OS are separated from the mineral fraction through a process known as pyrolysis. The pyrolysis of OS has heretofore generally been accomplished by one of two methods. The first method includes mining OS, crushing and then retorting or pyrolyzing the crushed OS in a fixed retorting plant or unit to retort the oil contained therein. The second recovery method is the retorting of the OS *in situ*, or in place, which eliminates the need for a retorting plant and its attendant apparatus [5]. During pyrolysis, kerogen is released from the mineral surface to which it is adsorbed and subsequently undergoes chemical transformations. This decomposition typically occurs without oxygen, under pressure and at operating temperatures above 450 °C [6]. Microwave technique is a potentially attractive technique as it provides a volumetric heating process at improved heating efficiencies in comparison with conventional techniques. If the microwave is controlled correctly, uniform heating within the material can be obtained. Heat is generated volumetrically within the material rather than from an external source [7]. The microwave frequency range lies between 300 MHz and 300 GHz, with most microwave applications falling between 3 and 30 GHz. In industry, microwave heating is performed at either a frequency close to 900 MHz or at 2450 MHz [8]. Microwave heating has long been employed in the food and rubber industries, but there is a growing interest for its potential use in other industrial processes, such as pyrolysis of oil shale [9–11], biomass [12], tires and plastics [13]. Microwave pyrolysis uses heat generated by microwaves to reach these temperatures in a fraction of the time of conventional heating technique.

OS is a complex polymeric material with a complicated porous structure that is difficult to classify. As it is known to us all, pore properties directly influence the inward and outward diffusion of oil vapor and gas and reactions within particles. In addition, as an important product of pyrolysis, semi-coke (SC) can be burnt directly to produce electricity or heat. The pore structure of SC is the critical physical property that affects pyrolysis, ignition, combustion, and burnout of SC [14]. The mechanism of OS microwave pyrolysis shows that physical structure of particle plays an important role during OS pyrolysis. Most of the studies have focused on determining the pore information of OS particles using gas adsorption/desorption, SEM, mercury intrusion, and drawn some conclusions [15–17]. Similar techniques have been applied to coal [18, 19] and char [20–22]. There are few reports about the surface characteristic of SC particle from microwave pyrolysis of OS and its change during pyrolysis.

In this study, microwave technology was employed to treat Jilin Huadian oil shale, and its semi-coke was analyzed by a scanning electron microscope.

The box-counting approach was introduced into SEM photograph analysis. At the same time, the surface fractal dimensions of OS/SC particles by FHH model calculation were obtained. The results showed that the final temperature and the pyrolysis power have a notable impact on the pore of semi-coke. In addition, the results of FHH model calculation were used to provide an authentication for the box-counting approach.

Experimental

Huadian OS

In this research, the raw OS was taken from the 4th layer of Dachengzi mine in Huadian city, China. It was dried, crushed and sieved to several size ranges of 0–6 mm (0–0.2, 0.2–1, 1–3, 3–6 mm), and then stored in desiccators before microwave pyrolysis. The proximate and ultimate analysis of the samples is as follows (%):

– Proximate analysis: M_{ad} 5.63, V_{ad} 25.46, A_{ad} 67.62, FC_{ad} 1.29, $Q_{net,ar}$ 5391 (J/g);

– Ultimate analysis: C_{ad} 18.25, H_{ad} 3.23, N_{ad} 0.58, O_{ad} 3.71, S_{ad} 0.98.

One can see that Huadian OS is a low-grade fuel with high content of ash and volatiles. It is unsuitable for long-distance transport, suiting for using near the site of discovery [23].

Experimental apparatus

Microwave pyrolysis apparatus

Pyrolysis by microwave radiation was performed using the experimental set-up shown in Fig.1. The microwave pyrolysis apparatus came from a modified microwave oven (Panasonic NN-GS575W) with incident power of

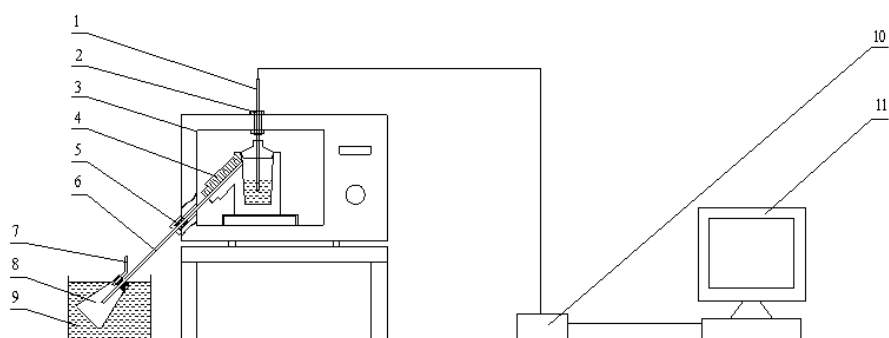


Fig. 1. Schematic diagram of oil shale microwave pyrolysis apparatus.

1 – thermocouple; 2 – fixed screw; 3 – microwave oven; 4 – silica container; 5 – microwave suppressor; 6 – education tube; 7 – non-condensing gas outlet pipe; 8 – conical flask; 9 – cooling tank; 10 – data collector; 11 – computer.

1000 W and operating at 2450 MHz. Agilent 34970 data collector (USA) was used to record temperature profile [24].

Scanning electron microscopy (SEM)

Scanning electron microscopy analysis was used to explore the structural transformations of OS/SC particles. The analysis was performed using Quanta 200 Environmental Scanning Electron Microscope made by FEI Company (Netherlands, resolution could reach at 3.5 nm at 30 kV). Samples were platinum-coated by a vacuum electric sputter coater to a finest thickness before the measurements.

Adsorption/Desorption isotherms measurement

Nitrogen adsorption/desorption at liquid nitrogen temperature ($-196\text{ }^{\circ}\text{C}$) was carried out on a Quantachrome Autosorb-1-C instrument (USA). Nitrogen adsorption at 77.3 K was measured at relative pressure P/P_0 of 0.05-0.986, where P and P_0 represent balance pressure and saturation pressure, respectively. The samples were outgases at $140\text{ }^{\circ}\text{C}$ and a final pressure of 0.334 MPa after two hours before the measurements.

Microwave pyrolysis procedure

The pyrolysis by microwave irradiation was conducted with a sample of 20 g of OS particles ($0.2\text{ mm} < \text{particle size} \leq 1\text{ mm}$), mixed with 2 g graphite powder to allow uniform heating, which was placed in a silica container. After application of microwave field, the sample was heated up immediately and rapidly to the desired final temperature. After a needed residence time, the microwave generator was stopped and the temperature was real-time measured with a chromel–alumel thermocouple. The system was then allowed to cool down to room temperature. Another sample was heated and cooled for each power and temperature.

Results and discussion

Fractal theory is one of the approaches of non-linear mathematics and has become increasingly popular in social and natural sciences as a means for characterizing intricate phenomena. Fractal theory makes it easy for quantitatively describing complex self-similar geometry, which is difficult with Euclid's geometry [25]. It has been proven that inner pore network [18, 19, 21] and particle surface [26] of coal have a fractal characteristic. The fractal dimension describes the complexities of pore shape. In general, higher fractal dimension indicates a more complex pore shape. The physical meaning of the pore fractal dimension during combustion is related to the gas diffusion within the pores. The pore structure of OS is a highly complex system. Its characteristics, which are irregularity, uncertainty, ambiguity and

self-similarity, reflect the pores' complexity comprehensively. Fractal geometry has gradually established its importance in the study of image characteristics. There are many techniques to estimate the dimensions of fractal surfaces. A famous technique to calculate a fractal dimension is the grid dimension approach popularly known as the box-counting approach [27].

Fractal processing of SEM image

Mandelbrot (1982) stated that one criterion of a surface being fractal is its self-similarity. Self-similarity can be explained as follows. Consider a bounded set A in Euclidean n -space. The set is said to be self-similar when A is the union of N_r distinct (non-overlapping) copies of itself each of which is similar to A scaled down by a ratio r . Fractal dimension D of A can be derived from the relation [28].

$$D = \log(N_r) / \log(1/r) \quad (1)$$

Eq. (1) is the basis of estimating the fractal dimension (FD) by the box-counting approach. Here, N_r is wing way. Assume that the image of size $M \times M$ pixels has been scaled down to a size $s \times s$ where $M/2 \geq s > 1$ and s is an integer. Then we know that $r = s/M$. Now, consider the image as a 3D space with (x, y) denoting 2D position and the third coordinate (z) denoting gray-level. The (x, y) space is partitioned into grids of size $s \times s$. On each grid, there is a column of boxes of size $s \times s \times s$. Let the minimum and maximum gray level of the image in the $(i, j)^{th}$ grid fall in the k^{th} and the l^{th} box, respectively. Then

$$n_{r(i,j)} = l - k - 1 \quad (2)$$

is the contribution of N_r in the $(i, j)^{th}$ grid. Taking contributions from all grids, we have

$$N_r = \sum_{i,j} n_r(i, j) \quad (3)$$

N_r is counted for different values of r (*i.e.* different values of s). Then using Eq. (1) we can estimate D , the fractal dimension, from the least-squares linear fit of $\log(N_r)$ against $\log(1/r)$ [29].

In this paper, Matlab is a platform compiler to calculate the fractal dimension of SEM image of SC, given in Fig. 2. During the calculation of fractal dimension, selection of the sub-image window needs to be considered. If sub-image window size is too small, it will be a significant loss of texture properties. If it is too large, the edge pixel and other pixel of an image region mixed to impact on the selection of texture features.

SEM image analysis of OS /SC samples

The aim of this section is to describe the results obtained from various conditions about the structure and morphological characteristics of OS/SC.

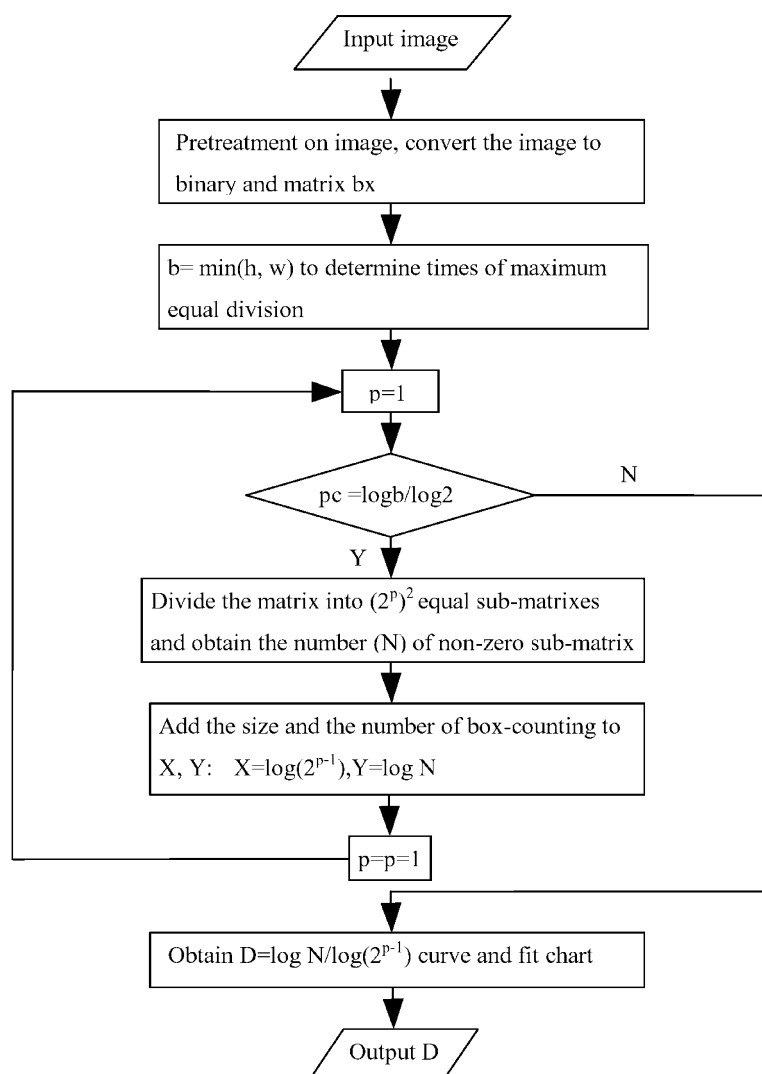
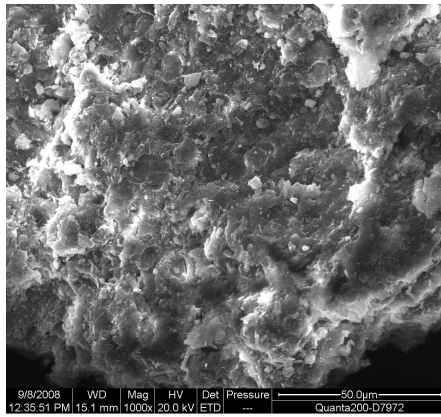


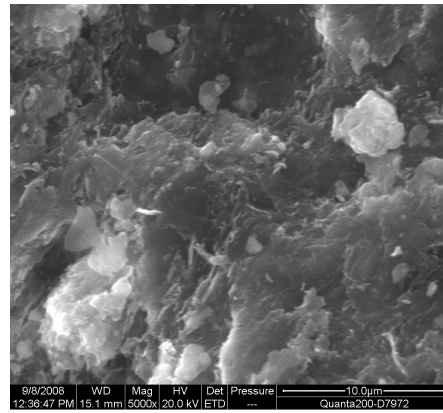
Fig. 2. Flowchart of the Matlab algorithm.

Influence of the microwave power

Figure 3 (a)–(e) shows SEM images of the raw OS and SC obtained from microwave pyrolysis under different microwave powers ($\pi_i = 400, 550, 700$ and 1000 W). The standard magnification of $1000\times$ and $5000\times$ are chosen because they give an adequate resolution of mesopores, and enable the operator to search out surface areas without too many fly ash particles or surface folds/irregularities. Ideally, the field of view should be covered by a flat smooth coke surface without fly ash. However, these are rarely the case, and unwanted features must be removed during the subsequent image processing. In some cases, parts of macro pores are present in the field of view and must be omitted from the measurement.

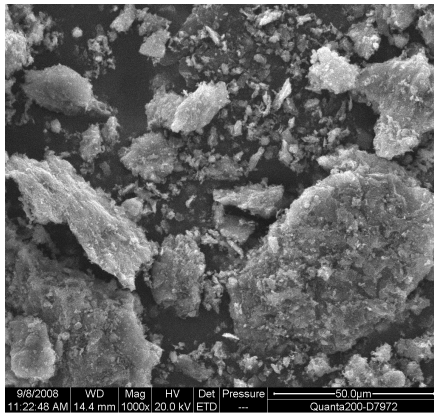


1000x

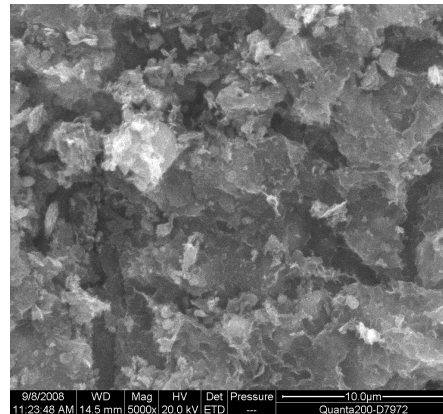


5000x

(a) raw OS

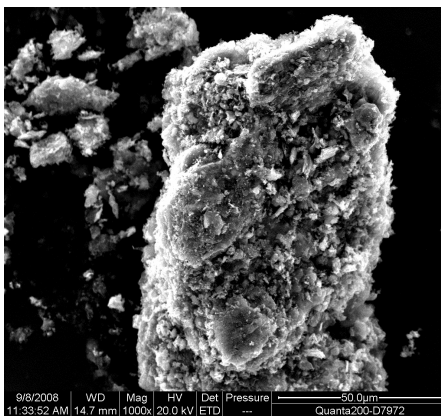


1000x

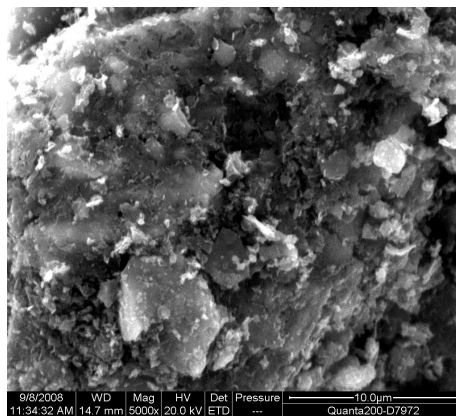


5000x

(b) $\pi_i = 400$ W



1000x



5000x

(c) $\pi_i = 550$ W

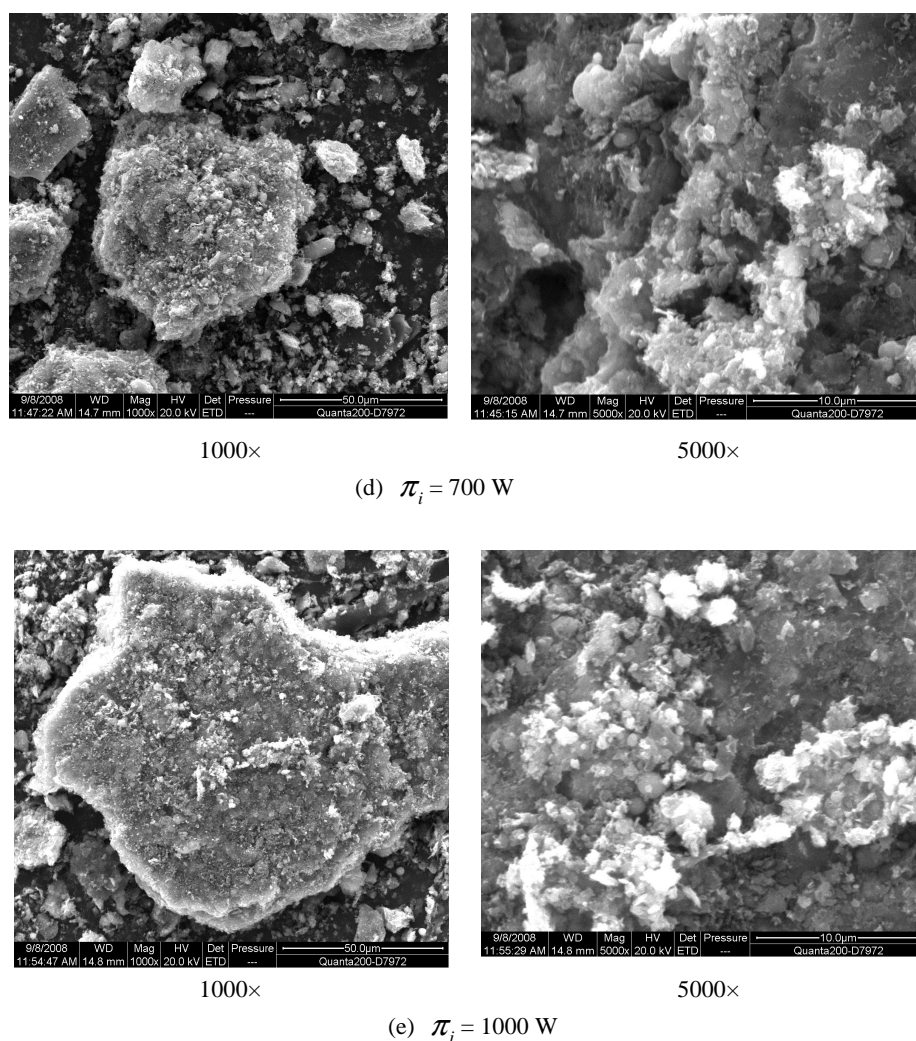


Fig. 3. SEM images of Huadian OS/SC under different input microwave power.

The SEM micrographs revealed the presence of sheets of organic matter on the grains of OS (Fig. 3 (a)). The surface of OS has pores of a certain degree, and the pore size is very irregular, but overall it shows a relative smooth surface comparing with the surface of SC samples.

With the increase of microwave power, the surface texture of SC becomes increasingly irregular due to the enlargement of porosity, which is caused by devolatilization. Evaporation of volatile material creates some pores on the particles. These characteristics are shown clearly in Fig. 3 (b). When the pyrolysis is performed at elevated powers ($\pi_i = 500$ and 700 W), the morphology of SC changes significantly and shows signs of increased degradation at the surface (Fig. 3 (c) and (d)). The larger pores contain multiple smaller pores within forming irregular spaces in the particle

(Fig. 3 (d)). Meanwhile, it also appears the possibility of fragmentation because several cracks passing through the particle can be seen clearly. The external surface is found covered mostly with smooth open pores of different sizes (Fig. 3 (e)) [30, 31].

Figure 4 presents the evolution of the fractal dimension with microwave powers ($\pi_i = 400, 550, 700$ and 1000 W). As it can be seen, the following observations are found.

With increasing the microwave power, the fractal dimension (D) of SC is improved, the surface structure moves towards larger complex, because the individual pore enlarges and pores have been coalesced to form a larger composite pores. The maximum fractal dimension detected in the analysis $\pi_i = 1000$ W. The fractal dimension of $\pi_i = 1000$ W is significantly greater than that of other groups ($\pi_i = 400, 550$ and 700 W).

Equilibrium temperature

Figure 5 shows the time dependence of the temperature during the pyrolysis of OS under microwave irradiation ($\pi_i = 550$ W). It is observed that the sample temperature increases and passes by a maximum at a time t_{\max} which depends on the applied microwave power ($t_{\max} = 330$ s). Beyond t_{\max} , the temperature decreases slightly and seems to level out around 845 °C independently of the power. As it is shown, the analysis of the curve is divided in three zones.

(1) In zone I, the heating of the material can be explained by dielectric relaxation phenomena of polar water molecules, which is responsible for the initial heating of the sample, leading to a faster increase in temperature and a subsequent decomposition of the organic and mineral matters during the degradation of the kerogen for temperatures corresponding to $t < t_{\max}$.

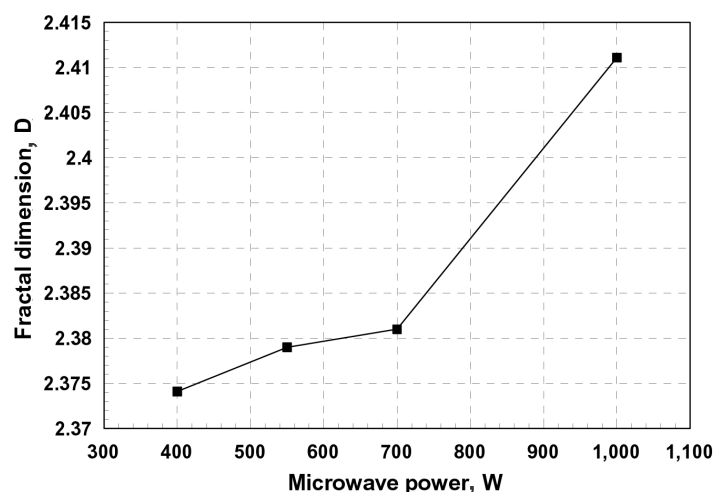


Fig. 4. The fractal dimension of SEM images for SC sample under different incident microwave power.

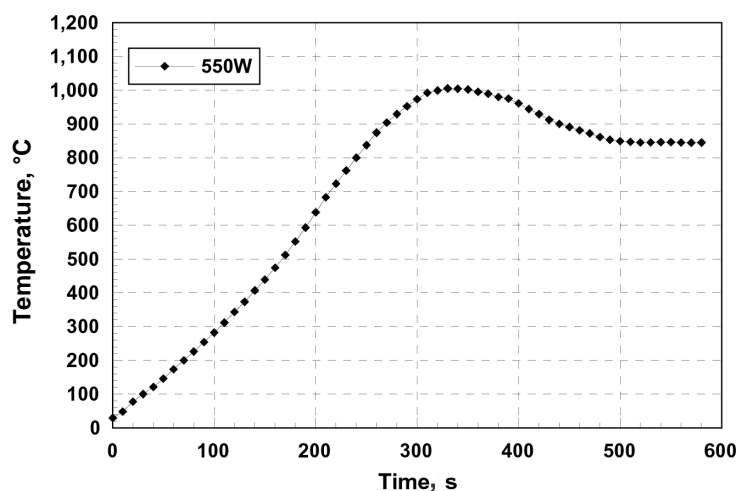


Fig. 5. Time dependence of the temperature during the pyrolysis of OS under microwave irradiation ($\pi_i = 550$ W).

(2) In zone II, the temperature decrease may result from the disappearance of water and the decrease in the products of the pyrolysis as well as the decomposition of pyrite. This may also result from endothermic reactions that may occur in this zone as the maximum temperature is greater than that needed for the decomposition of carbonates.

(3) In zone III, the temperature is stable at about 845 °C. This may result from the relaxation of the products of the decomposition of zone III, the temperature is stable at about 845 °C. This may result from the relaxation of the products of the decomposition of the mineral matrix, the compounds formed by reactions between the different constituents and the pyrolysis of residues [11].

In addition, the equilibrium temperature is different under various incident microwave power ($\pi_i = 400$ W; $T_e = 809$ °C; $\pi_i = 550$ W, $T_e = 845$ °C; $\pi_i = 700$ W, $T_e = 870$ °C; $\pi_i = 1000$ W, $T_e = 906$ °C), and it is found to increase with incident microwave power, given in Fig. 6.

Effects of the final temperature

Figure 7 presents the SEM pictures of SC of the same microwave power ($\pi_i = 550$ W) for final temperatures $T = 400, 520, 700, 900$ °C and equilibrium temperature (T_e). As it can be seen, the final temperature of microwave pyrolysis has a significant influence on the microstructure. The main performance is the increase of the number of pore and the change of the size of pore. As a result of OS particles subject to thermal stress, the higher the temperature, the more the surface of SC particle prone to crack and pore. Meanwhile, the increase of volume and the escape rate of volatiles are also promoting the development of particle porosity. There are many physical

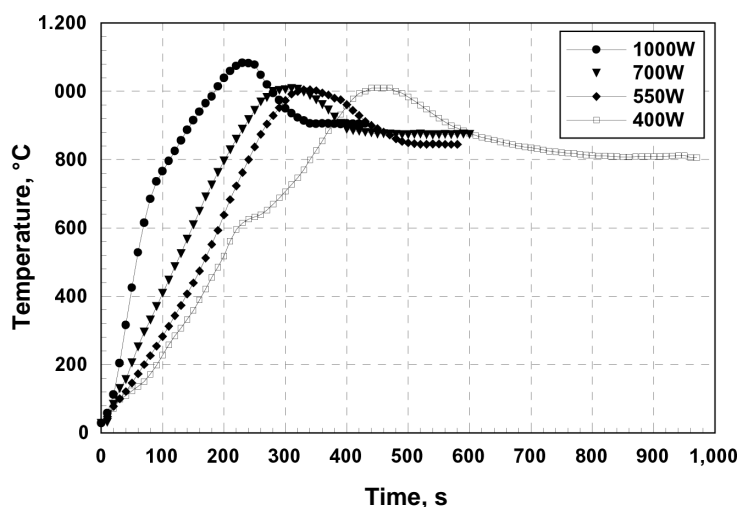


Fig. 6. Time dependence of the temperature during the pyrolysis of OS under different microwave irradiation.

and chemical phenomena during pyrolysis, including plasticity and depolymerization. These phenomena affect the structure of SC pore, especially for OS with high content of ash and volatiles. Recent studies show that SC reactivity and pyrolysis conditions are related through the structural evolution and morphological changes.

1. When the temperature is below 500 °C (Fig. 7 (a)), evaporation of volatile material creates some pores with a rough surface and irregular outlet. The pore volume does not change significantly up to the temperature of softening.

2. With the development of reaction, a large number of volatile materials would be released from the depths of OS and the tar would be formed. Evaporation of volatile material creates some pores on the particle with the rough surface and irregular outlet (see Fig. 7 (b) and (c)).

3. When the pyrolysis is performed at an elevated temperature ($T = 900$ °C), which promotes the increase of carbonization, the tar and volatile material are released rapidly. While micro pores are expanded into meso pores, meso pores are also expanded into the macro pores (see Fig. 7 (d)).

4. When the temperature is above 1000 °C (Fig.7 (e)), multiple smaller pores would be performed because the lighter volatile material continues to be released. However, the transformations are rapid and the morphological observation of the residues showed aggregates of fused grains.

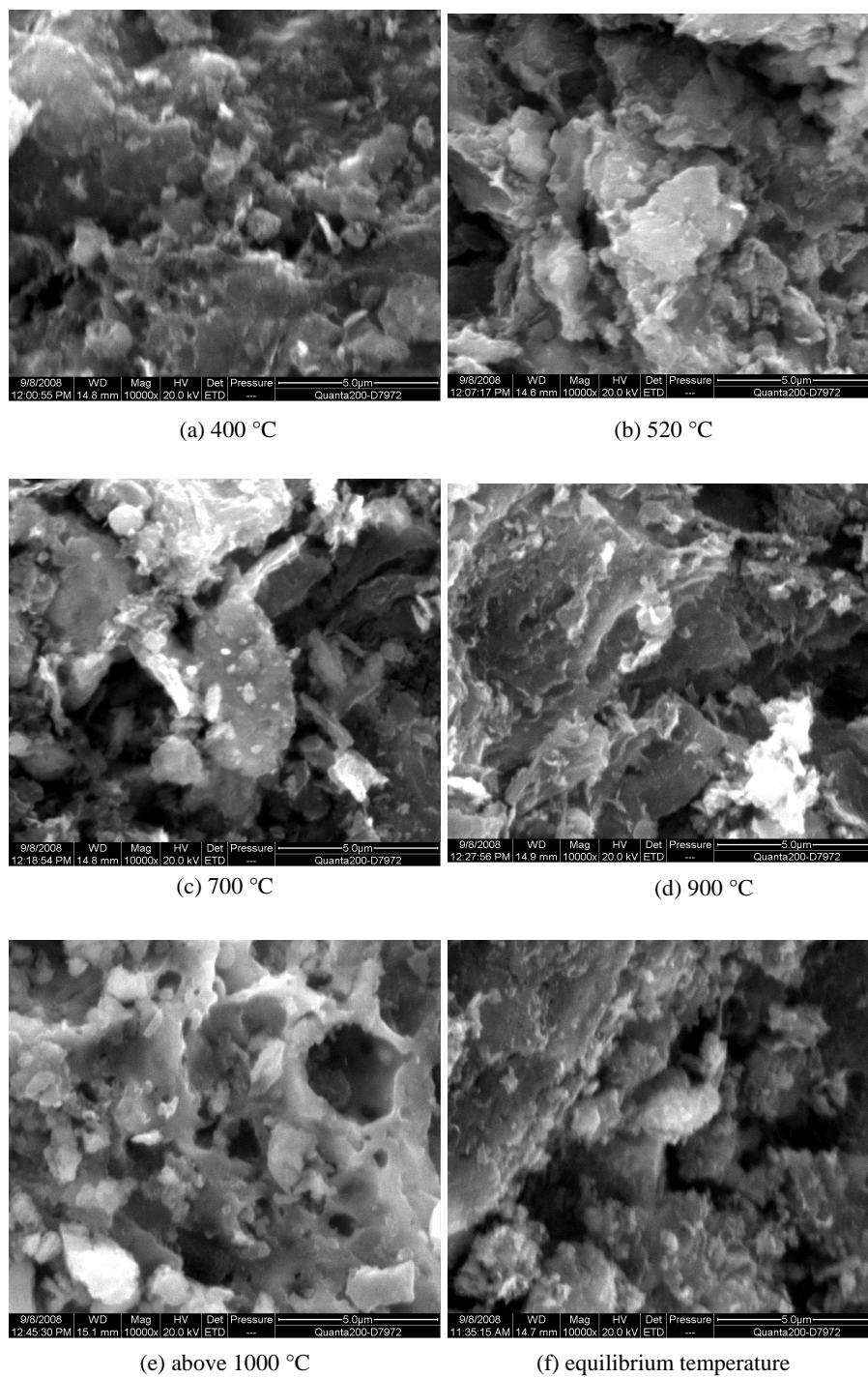


Table 1. The fractal dimension of the SEM images under different final temperatures

Final temperature of OS pyrolysis, °C	Box-counting dimension, D
ambient (raw OS)	2.271
400	2.2892
520	2.3587
700	2.3631
900	2.4233
Equilibrium temperature	2.3790

The box dimension of SEM images ($\pi_i=550$ W) under different final temperature ($T=0, 400, 520, 700, 900$ °C and equilibrium temperature) is shown in Table 1. From the figures, the following observations were found:

1. The higher the final temperature, the greater the fractal dimension on the surface of SC structure.

2. The fractal dimension of $T=900$ °C sample is 2.4233, arrives at maximum, then decreases slowly. At the same time, the expansion degree of sample spatial structure is the strongest.

3. When the temperature reaches equilibrium temperature (T_e), the box dimension of SC has decreased, but still greater than that at 700 °C. However, we can find that a number of pore structures are destroyed by the melt of the carbocool in the high temperature.

FHH model approach

In order to confirm the results above and to elucidate the role of the relaxation losses of these molecules as the precursor for microwave pyrolysis the material and the subsequent degradation of the organic matter, we have performed another experiment (FHH model approach) at the same conditions ($\pi_i=400, 550, 700$ and 1000 W; $T=400, 520, 700, 900$ °C and equilibrium temperature).

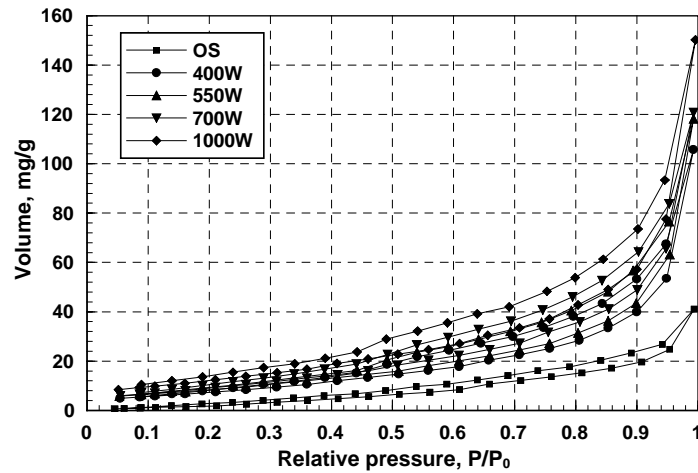
Fractal geometry has been widely used in many areas of modern science. The key quantity of the fractal geometry is the fractal dimension D , which is an operative measure of the surface and structural irregularities of a given solid. The concept of fractality introduced by Mandelbrot [28] was applied for the first time by Avnir and Pfeifer [32] to characterize the degree of complexity of a surface material from adsorption-desorption data. Since this pioneer work, many materials having a complex structure have been claimed as fractal. One way to define the fractal dimension D is an adaptation of the Frenkel-Halsey-Hill (FHH) theory of multilayer adsorption to the fractal surfaces. The experimental approaches used for the determination of the surface fractal dimension of porous solids have been reviewed by Avnir et al.

$$a = k[\ln(p_o / p)]^{D-3}. \quad (4)$$

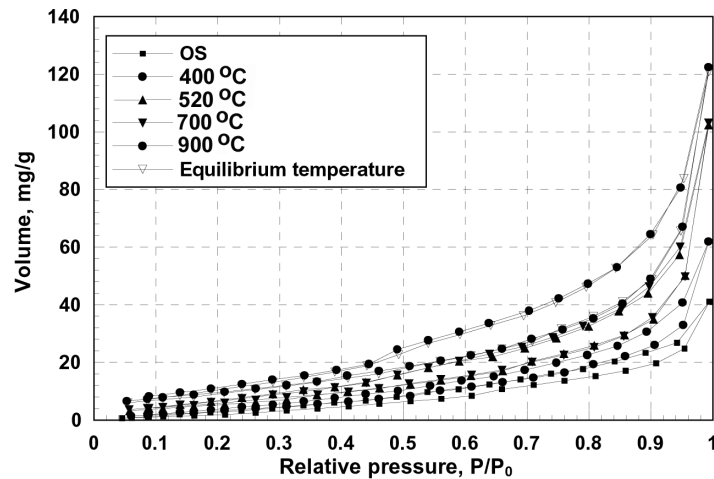
Eq. (4) is changed into a logarithmic form

$$\ln a = (D - 3) \ln \ln(p_o / p) + C \quad (5)$$

where a is the amount adsorbed at the relative pressure p / p_o , C is constant. According to the fractal FHH model (Eq. (5)), on the plot of $\ln a$ vs. $\ln \ln(p_o / p)$, the slope of the straight-line portion should equal $D - 3$. So, D values can be obtained.



(a) Different microwave incident power



(b) Different final temperature

Fig. 8. Adsorption/desorption isotherms of OS/SC under different working conditions.

Effects of the microwave power

Figure 9 shows the adsorption data fitting chart of SC of the same equilibrium temperature (T_e) for microwave incident power $\pi_i = 400, 550, 700$ and 1000 W in accordance with the FHH model. Their correlation coefficient values are greater than 0.99. Figure 10 shows the fractal dimension under different microwave incident power ($\pi_i = 400, 550, 700$ and 1000 W). The analysis of these results shows that the fractal dimensions of SC samples are increased with improvement of the microwave power. But, fractal dimension of SC samples of $\pi_i = 400$ W, 550 W and 700 W

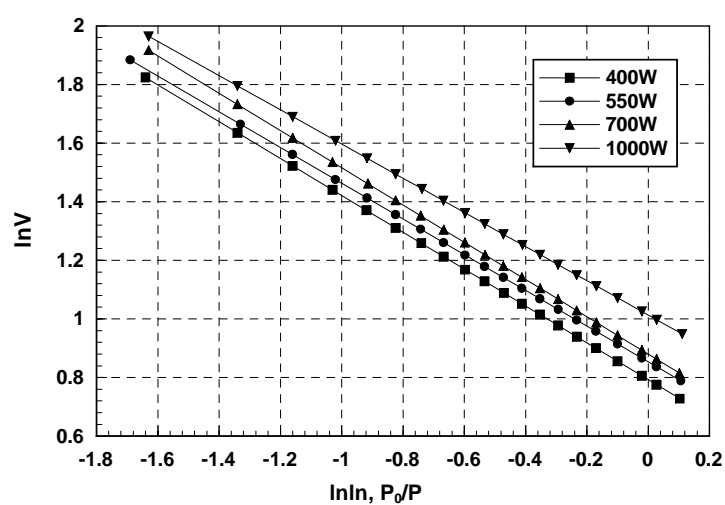


Fig. 9. Fitting chart of SC under different microwave power.

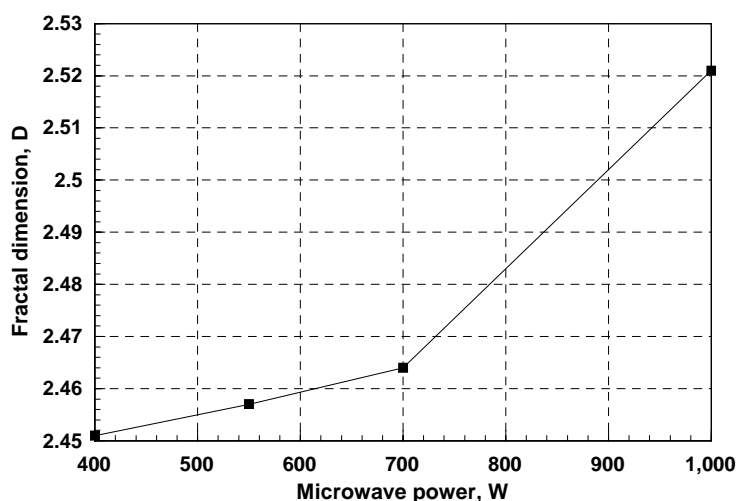


Fig.10. Fractal dimension of SC samples under different microwave power.

differed indistinctly ($D = 2.451, 2.457$ and 2.464). The fractal dimension of $\pi_i = 1000$ W is 2.521, which is higher than the previous. The results also confirm that the analysis of SEM pictures presented above (next Section).

Effects of the final temperature

Figure 11 shows the fitting chart of SC at the same microwave power ($\pi_i = 550$ W) for final temperature $T = 400, 520, 700, 900$ °C and equilibrium temperature in accordance with the FHH equation, and the correlation coefficient values are greater than 0.99. Table 2 shows the fractal dimension of SC samples under different final temperatures. As it is shown, the fractal FHH model dimension is divided into three groups:

(1) In the group I, the fractal dimensions of OS and SC of $\pi_i = 400$ °C are 2.318 and 2.333, respectively. It appears that the specific pore volume does not change significantly with final temperature in the range of pore size < 2 nm, indicating that the final temperature has little influence on the development of micro pores.

(2) In the group II, the fractal dimensions of SC of $\pi_i = 520$ °C and 700 °C are 2.395 and 2.415, respectively. The results show that many volatiles inside particles have escaped in the temperature range of 520 – 700 °C, lots of new pores are generated. Above 700 °C, the dielectric constant of the oil shale increases sharply with temperature, and the receptivity of microwave energy become stronger. Therefore, the volatiles inside particles erupt out greatly and rapidly, and new pores are generated and original pores are enlarged.

(3) In the group III, the fractal dimensions of SC of $\pi_i = 900$ °C and equilibrium temperature are 2.475 and 2.464, respectively. Above 900 °C, some small molecules may still escape, resulting in producing new pores.

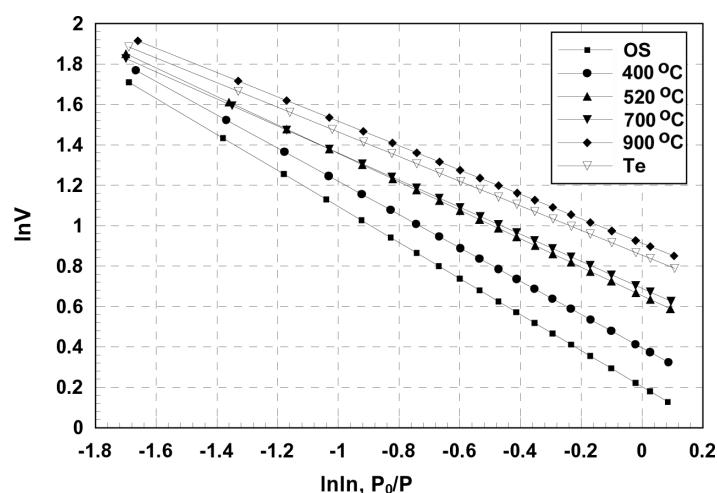


Fig. 11. Fitting chart of SC under different final temperature.

However, before arriving at the equilibrium temperature (T_e), the maximum temperature can reach about 1000 °C. At 1000 °C, samples will soften and deform, which leads to reduction of the pore radius or even closing some pores. Therefore, the specific surface area and specific pore volume of SC of $\pi_i = 900$ °C are more than that of the equilibrium temperature.

In contrast to the above analysis, we can find that the pore structure changes of samples are objectively characterized by the fractal dimension during the microwave pyrolysis process.

Table 2. Fractal dimension of SC samples under different microwave incident power

Final temperature of OS pyrolysis, °C	FHH model dimension, D
ambient (raw OS)	2.318
400	2.333
520	2.395
700	2.415
900	2.475
Equilibrium temperature	2.464

Box-counting approach comparison with FHH approach

The test results (Table 3) after modeling to FHH model and box-counting model indicate that the box-counting dimension of SEM images is little less than the FHH model dimension, because SEM cannot take the images of SC inner pore. Their error rate is within 5%, and the testing data are credible.

Table 3. Comparison of FHH model dimension and box-counting dimension

		FHH model dimension	Box-counting dimension
Final temperature, °C	raw OS	2.318	2.271
	400	2.333	2.289
	520	2.395	2.359
	700	2.415	2.363
	900	2.475	2.423
Power, W	400	2.451	2.374
	550	2.457	2.379
	700	2.464	2.381
	1000	2.521	2.411

Conclusions

1. The fractal dimension could be used to estimate the fractal pore structure characteristics of OS/SC.
2. The input power and the final temperature have a significant impact on the micro-structure of samples during the process of OS microwave pyro-

lysis. The higher the microwave incident power, the more disorder on the surface of SC particle sample. As a result of OS particles subject to thermal stress, the higher the temperature, the more the surface of SC particle prone to crack and pore.

3. The analysis of FHH model dimension results show that the fractal dimension of samples improved with increasing the microwave input power and final temperature. The variation regularity of FHH model dimension is consistent with the box-counting dimension.
4. The box-counting dimension of SEM images is little less than FHH model dimension, which is attributed to that SEM cannot take the images of SC particle inner pore.

Acknowledgments

The authors are grateful for financial support from the National Natural Science Foundation of China (Grant 50876018) and the Key Project of Research Program of Jilin Province (20075015).

REFERENCES

1. Revue Internationale Europe Outremer. 1982; 627: 14.
2. Qian, J. L., Wang, J. Q., Li, S. Y. Oil shale development in China // Oil Shale. 2003. Vol. 20, No. 3S. P. 356–359.
3. Williams, P. T., Ahmad N. Investigation of oil-shale pyrolysis processing condition using thermogravimetric analysis // Appl. Energ. 2000. Vol. 66, No. 2. P. 113–133.
4. Qing, W., Baizhong, S., Xiahua, W., Jingru, B., Jian, S. Influence of retorting temperature on combustion characteristics and kinetic parameters of oil shale semicoke // Oil Shale. 2006. Vol. 23, No. 4. P. 328–339.
5. Ellington, R. T. Method of Retorting Oil Shale in Situ. US Patent 3586377 (1971).
6. Qing, W., Baizhong, S., Xiahua, W., Jingru, B., Jian, S. Study on combustion characteristics of mixtures of Huadian oil shale and semicoke // Oil Shale. 2007. Vol. 24, No. 2. P. 135–145.
7. Appleton, T. J., Colder, R. I., Kingman, S. W., Lowndes, I. S., Read, A. G. Microwave technology for energy-efficient processing of waste // Appl. Energ. 2005. Vol. 81, No. 1. P. 85–113.
8. Meredith, R. J. Engineers' Handbook of Industrial Microwave Heating. - London: Institution of Electrical Engineers, 1998.
9. Ben Chanaa, M., Lallemand, M., Mokhlisse, A. Pyrolysis of Timahdit, Morocco, oil shales under microwave field // Fuel. 1994. Vol. 73, No. 10. P. 1643–1649.
10. Bradhurst, D. H., Worner, H. K. Evaluation of oil produced from the microwave retorting of Australian shales // Fuel. 1996. Vol. 75, No. 3. P. 285–288.

11. *El Harfi, K., Mokhlisse, A., Chanaa, M. B., Outzourhit, A.* Pyrolysis of the Moroccan (Tarfaya) oil shales under microwave irradiation // *Fuel*. 2000. Vol. 79, No. 7. P. 733–742.
12. *Dominguez, A., Menendez, J. A., Fernandez, Y., Pis, J. J., Nabais, J. M. V., Carrott, P. J. M., Carrott, M. M. L.R.* Conventional and microwave induced pyrolysis of coffee hulls for the production of a hydrogen rich fuel gas // *J. Anal. Appl. Pyrol.* 2007. Vol. 79, No. 1–2. P. 128–135.
13. *Sun, B. Z., Wang, Q., Li, S. H., Wang, H. G.* Analysis of specific area and porous structure of oil shale and semi-coke // *Journal of Power Engineering*. 2008. Vol. 28, No. 1. P. 163–167 [in Chinese].
14. *Cranston, R. W., Inkley, F. A.* The determination of pore structures from nitrogen adsorption isotherms // *Advances in Catalysis*. – New York: Academic Press Inc, 1957. Vol. 9. P. 143–154.
15. *Tisot, P. R.* Properties of Green River oil shale determined from nitrogen adsorption and desorption isotherms // *J. Chem. Eng. Data*. 1962. Vol. 7, No. 3. P. 405–410.
16. *Slettevold, C. A., Biermann, A. H., Burnham, A. K.* LLNL Report UCRL-52619. – Livermore, CA, 1978.
17. *Schrodt, J. T., Comer, A. C.* Surface Area and Pore Volume Distributions of Eastern US Oil Shales // *European Federation of Chemical Engineers, Conference on Energy*, London, UK, 1982, P. A/51–A/56.
18. *Nakagawa, T., Komaki, I., Sakawa, M., Nishikawa, K.* Small angle X-ray scattering study on change of fractal property of Witbank coal with heat treatment // *Fuel*. 2000. Vol. 79, No. 11. P. 1341–1346.
19. *Sastry, P. U., Sen, D., Mazumder, S., Chandrasekaran, K. S.* Structural variations in lignite coal: a small angle X-ray scattering investigation // *Solid State Commun.* 2000. Vol. 114, No. 6. P. 329–333.
20. *He, R., Xu, X., Chen, C., Fan, H., Zhang, B.* Evolution of pore fractal dimensions for burning porous chars // *Fuel*. 1998. Vol. 77, No. 12. P. 1291–1295.
21. *Diduszko, R., Swiatkowski, A., Trznadel, B. J.* On surface of micropores and fractal dimension of activated carbon determined on the basis of adsorption and SAXS investigations // *Carbon*. 2000. Vol. 38, No. 8. P. 1153–1162.
22. *Saito, K., Komaki, I., Hasegawa, K. I., Tsuno, H.* In-situ variable-temperature single-point NMR imaging study of coals // *Fuel*. 2000. Vol. 79, No. 3–4. P. 405–416.
23. *Qing, W., Baizhong, S., Aijuan, H., Jingru, B., Shaohua, L.* Pyrolysis characteristics of Huadian oil shales // *Oil Shale*. 2007. Vol. 24, No. 2. P. 147–157.
24. *Wang Qing, Huan Xiankun, Liu Hongpeng, Sun Baizhong, Jia Chunxia.* Microwave induced pyrolysis of Huadian oil shale // *Journal of Chemical Industry and Engineering*. 2008. Vol. 59, No. 5. P. 1288–1292 [in Chinese].
25. *Falconer, K.* *Fractal Geometry: Mathematical Foundations and Applications*. New York: Wiley, 1990.
26. *Youzhong, R., Jian, F., Zhibo, C., Yuanquan, C.* Electron microscopic analyses of char structure and its fractal description // *Combust. Sci. Technol.* 1996. Vol. 2, No. 1. P. 9–14.
27. *Bisoi, A. K., Mishra, J.* On calculation of fractal dimension of images // *Pattern. Recogn. Lett.* 2001. Vol. 22, No. 6–7. P. 631–637.
28. *Mandelbrot, B. B.* *The Fractal Geometry of Nature*. – San Francisco: Freeman, 1982.

29. Chaudhuri, B. B., Sarkar, N. Texture segmentation using fractal dimension // IEEE T. Pattern. Anal. 1995. Vol. 17, No. 1. P. 72–77.
30. Song, H., Xiang, J., Sun, L., Xu, M., Qiu, J., Fu, P. Characterization of char from rapid pyrolysis of rice husk // Fuel Process. Technol. 2008. Vol. 89, No. 11. P. 1096–1105.
31. Bilali, L., Benchanaa, M., El harfi, K., Mokhlisse, A., Outzourhit, A. A detailed study of the microwave pyrolysis of the Moroccan (Youssofia) rock phosphate // J. Anal. Appl. Pyrol. 2005. Vol. 73, No. 1. P. 1–15.
32. Avnir, D., Pfeifer, P. Fractal dimension in chemistry: An intensive characteristic of surface irregularity // Nouv. J. Chim. 1983. Vol. 7, No. 2. P. 71–72.

Presented by Jialin Qian

Received December 3, 2009